JACS
JOURNAL OF THE AMERICAN CHEMICAL SOCIETY

ARTICLE

pubs.acs.org/JACS

Hole Injection/Transport Materials Derived from Heck and Sol−Gel Chemistry for Application in Solution-Processed Organic Electronic Devices

Younhee Lim,[†] Young-Seo Park,[‡] Yerang Kang,[†] Do Young Jang,[†] Joo Hyun Kim,[§] Jang-Joo Kim,*[,‡] Alan Sellinger,*[,∥] and Do Y. Yoon*[,†]

[†]Department of Chemistry, Seoul National University, Seoul 151-747, Korea

[‡]Department of Materials Science and Engineering, Seoul National University, Seoul 151-742, Korea

[§]Department of Polymer Engineering, Pukyong National University, Busan 608-739, Korea

[∥]Department of Material Science and Engineering and the Center for Advanced Molecular Photovoltaics (CAMP), Stanford University, Stanford, California 94305, United States

Supporting Information

ABSTRACT: An organosilicate polymer, based on *N*,*N*′-diphenyl-*N*,*N*′-bis(4-((*E*)-2-(triethoxysilyl)vinyl)phenyl)biphenyl-4,4′-diamine (TEVS-TPD) with extended conjugation between the Si atom and the aromatic amine, was prepared under mild conditions via sequential Heck and sol−gel chemistry and used as an alternative to poly(3,4-ethylenedioxythiophene):poly(styrenesulfonate) (PEDOT:PSS), the most widely used planarizing hole injection/transport layer in solution-processed organic electronic devices. Spin-coating TEVS-TPD polymer solutions yield defect-free, uniform, thin films with excellent adhesion to the ITO electrode. Upon thermal cross-linking at 180 °C, the cross-linked polymer exhibits excellent solvent resistance and electrochemical stability. Solution-processed organic light emitting diode (OLED) devices using iridium-based triplet emitting layers and cross-linked TEVS-TPD films as a hole injection/transport layer show significantly improved performance including lower leakage current, lower turn-on voltage, higher luminance, and stability at high current density, as compared to the control device prepared with PEDOT:PSS.

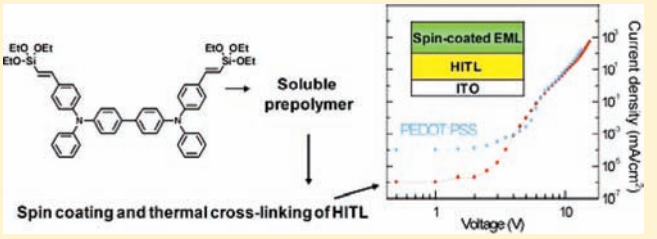

I. INTRODUCTION

Organic light emitting diodes (OLEDs) and organic photovoltaic solar cells (OPVs) critically depend on the hole injection/transport layers which, in addition to their main function to transport charges, also serve to planarize the often relatively rough surfaces of indium−tin−oxide (ITO) electrodes. Although not originally designed for this purpose, water-dispersed poly(3,4-ethylenedioxythiophene):poly(styrenesulfonate) (PEDOT:PSS) has been widely used for this application because it has an appropriate energy level for hole injection and transport characteristics, as well as the planarization capability. Moreover, the deposited PEDOT:PSS film is completely insoluble in organic solvents, which is essential to the solution processing of multilayer organic electronic devices such as polymer light emitting diodes (PLEDs) and OPVs. However, PEDOT:PSS has some shortcomings such as exciton quenching, anode corrosion, degradation of adjacent active polymeric layers, and weak interface adhesion,[1−6] which raise serious questions concerning the long-term device stability. Furthermore, the corrosive nature of the water-based PEDOT:PSS solutions are known to degrade print-head cartridges and inkjet nozzles when depositing by inkjet print methods. To overcome such problems, there have been extensive studies to prepare alternative planarizing hole injection/transport layers (HITLs) mainly focused on cross-linkable polymers, because insoluble layers are easily obtained via in situ cross-linking of solution-deposited films. In this regard, photocross-linkable polymers containing oxetane,[7,8] acrylate,[9,10] and cinnamic-functionalized groups[11] have been shown to be effective to a certain extent. In addition, thermally cross-linkable polymers containing trifluorovinylether,[12−15] cyclobutene,[16] vinyl groups,[17−19] and siloxanes[20,21] have been investigated to prepare all solution-processed multilayer PLEDs. In particular, organosilicate derivatives have been shown to render good adhesion properties to the inorganic ITO anode surface and good compatibility with the adjacent organic layer due to their organic−inorganic hybrid nature.[20−27] Recently, Marks et al. demonstrated that self-assembling monomers of trichlorosilylalkyl/trimethoxysilylalkyl functionalized aromatic amines such as *N*,*N*,*N*′,*N*′-tetraphenyl-1,1′-biphenyl-4,4′-diamine (TPD) exhibited good hole injection and transport performance in small molecule-based OLEDs[22−27] and PLEDs.[20,21] Despite the significant advances resulting from such extensive efforts, there is still a strong need for an improved material that can outperform the currently used PEDOT:PSS with regard to important device properties

Received: July 12, 2010
Published: December 30, 2010

dx.doi.org/10.1021/ja1061517 | *J. Am. Chem. Soc.* 2011, 133, 1375–1382

Scheme 1. Synthesis of TEVS-TPD Monomer and Initial Polymer[a]

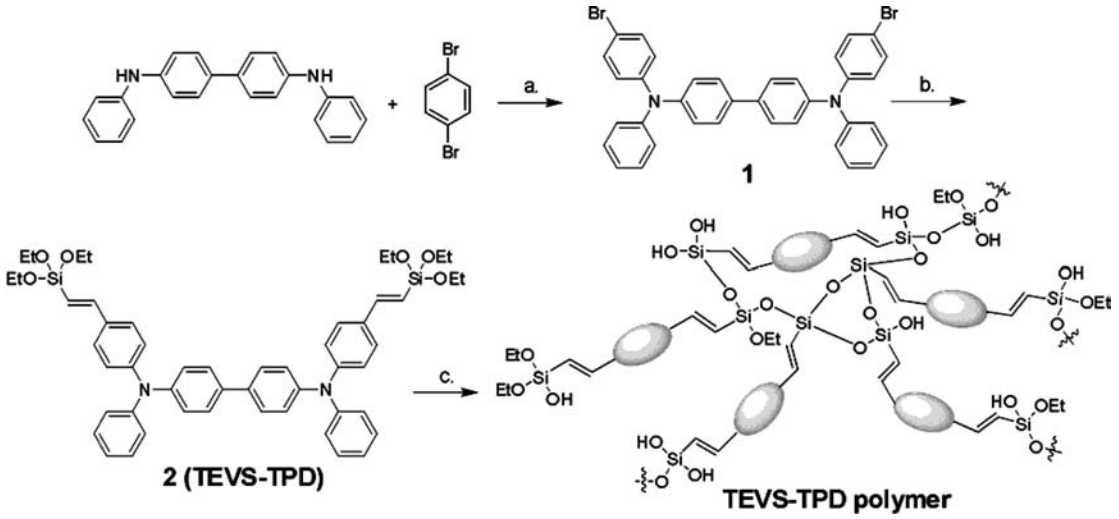

[a] (a) $Pd_2(dba)_3$, dppf, NaO*t*Bu, toluene, 90 °C, 10 h, 68% yield; (b) vinyltriethoxysilane, $Pd[P(tBu)_3]_2$, dicyclohexylmethylamine, dioxane, 80 °C, 10 h, 63% yield; (c) HCl, H_2O, THF, 60 °C, 2 h, >95% yield.

such as turn-on voltage, efficiency (cd/A, lm/W), brightness levels (cd/m^2), and most importantly device lifetime. Furthermore, the process to prepare such new materials must be straightforward involving simple chemistry for scalable processes and provide materials with a long shelf life and easy use.

In this Article, we report the preparation and device performance of a thermally cross-linkable organosilicate polymer with aromatic amine substituents as an improved alternative to PEDOT:PSS for application in OLEDs and OPVs. In comparison with previous studies that emphasized the self-assembly of monomer-type aromatic amine organosilicates, our work emphasizes soluble, branched organosilicate polymers for preparing defect-free, uniform, thin films by simple solution processing. Most importantly, triethoxysilane groups are attached straightforwardly by a mild Heck reaction[28,29] instead of traditional methods that use organomagnesium or butyllithium.[30] Moreover, this procedure to attach triethoxysilane groups introduces extended conjugation between the Si atom and the aromatic amine portion, instead of the insulating alkylsiloxane linkage in previous reports.[20−27] This extended conjugation will improve the hole injection/transport by decreasing the content and size of charge blocking moieties that impede efficient hopping of charges.

II. EXPERIMENTAL SECTION

Materials. Vinyltriethoxysilane was purchased from TCI. All other reagents were purchased from Sigma-Aldrich and used as received unless otherwise indicated. All the reagents were used without further purification. Toluene and 1,4-dioxane were distilled over sodium before use.

Experimental Methods. ^1H NMR and ^{13}C NMR spectra were recorded using a Bruker Advanced 300 MHz spectrometer. The molar masses of TEVS-TPD monomer and the polymer (see Scheme 1) were determined by a MALDI-TOF mass spectrometer (from Bruker Daltonics) and gel permeation chromatography (GPC) calibrated with polystyrene standards (Polymer Standard Service USA, Inc.), respectively. The GPC setup was comprised of two Agilent PLgel Mixed-D GPC columns, a Waters 2410 differential refractometer, and a Viscotek 270 viscometer/refractive index dual detector. Tetrahydrofuran (THF) was used as an eluent at a flow rate of 1.0 mL/min. Thermogravimetric analysis (TGA) and differential scanning calorimetry (DSC) measurements were carried out on a TGA Q50 and DSC 2910 (TA Instruments), respectively, with a heating rate of 5 °C/min. UV−vis absorption and photoluminescence (PL) spectra of the initial and the thermally cured films spin-coated on quartz plates were recorded with a JASCO V-530 UV−vis spectrophotometer and a JASCO FP-6500 spectrofluorometer, respectively. FT-IR spectra of the initial polymer and the cured polymer films spin-coated on silicon wafers were obtained using a JASCO 660 Plus FT-IR spectrometer. Cyclic voltammetry was performed using indium tin oxide (ITO) as the working electrode, Ag/Ag^+ as the reference electrode, and Pt wire as the counter electrode at a scan rate of 100 mV/s. 0.1 M tetrabutylammonium hexafluorophosphate (TBAPF) in acetonitrile was the electrolyte. The redox potentials (E_{ox} and E_{red}) were calibrated by using ferrocene (Fc) as the standard, whose HOMO energy level is −4.8 eV. Atomic force microscopy (AFM) images were obtained on a NanoScope III AFM in the tapping mode. Thickness of the layers were measured with Alpha step IQ (KLA Tencor). The OLED device characteristics were investigated using a Keithley 2400 programmable source meter and a SpectraScan PR650. The current−voltage data of organic thin film transistor (OTFT) devices were obtained using a Keithley 4200-SCS semiconductor parameter analyzer in ambient air at room temperature.

Synthesis of *N,N′*-Diphenyl-*N,N′*-bis(4-bromophenyl)-biphenyl-4,4′-diamine (TPD-Br2, 1). Tris(dibenzylideneacetone)-dipalladium ($Pd_2(dba)_3$, 0.687 g, 0.750 mmol) and diphenylphosphinoferrocene (dppf, 0.626 g, 1.13 mmol) were dissolved in dry toluene under argon atmosphere. After 1,4-dibromobenzene (23.4 g, 0.100 mol) was added, the reaction mixture was stirred for 10 min. To the mixture were added sodium-*tert*-butoxide (6.01 g, 62.5 mmol) and *N,N′*-diphenylbenzidine (8.41 g, 25.0 mmol). The reaction mixture was heated at 90 °C overnight and deemed complete via thin layer chromatography (TLC) analysis. After being cooled to room temperature, the mixture was filtered through Celite and washed with toluene and water. The organic layer was extracted with toluene (100 mL × 3) and dried over $MgSO_4$. The solvent was evaporated on a rotary evaporator, and the dark brown mixture was purified by column chromatography on silica gel using methylene chloride/*n*-hexane (1:6) as eluent to give a white solid (R_f: 0.3). Yield: 11 g (68%). ^1H NMR ($CDCl_3$, δ): 7.45 (d, 4H, J = 8.53 Hz), 7.34 (d, 4H, J = 8.76 Hz), 7.27 (t, 4H, J = 8.20 Hz), 7.12−7.03 (m, 10H), 6.99 (d, 4H, J = 8.63 Hz). ^{13}C NMR ($CDCl_3$, δ): 147.23, 146.87, 146.36, 135.13, 132.22, 129.44, 127.49, 125.32, 124.56, 124.32, 123.41, 114.99.

dx.doi.org/10.1021/ja1061517 |*J. Am. Chem. Soc.* 2011, 133, 1375–1382

Scheme 2. Structure of TEPCS-TPD Monomer

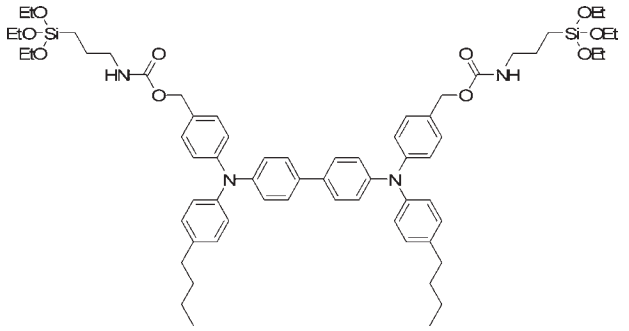

Synthesis of *N,N′*-Diphenyl-*N,N′*-bis(4-((*E*)-2-(triethoxysilyl)-vinyl)phenyl)biphenyl-4,4′-diamine (TEVS-TPD, 2). To a flame-dried round-bottom flask were added **1** (4.01 g, 6.20 mmol), bis(tri*tert*-butylphosphine)palladium ($Pd[P(tBu)_3]_2$, 0.063 g, 0.12 mmol), and dry dioxane (30 mL). To the reaction mixture, vinyltriethoxysilane (3.25 mL, 15.4 mmol) and argon degassed dicyclohexylmethylamine (3.3 mL, 15.4 mmol) were added. The mixture was stirred at 80 °C overnight under argon atmosphere and deemed complete by TLC analysis. After being cooled to room temperature, the reaction mixture was filtered and the filtrate concentrated on a rotary evaporator. The crude mixture was subsequently dissolved in ethyl acetate and washed with cold 5% HCl three times and with water twice. The organic layer was dried over Na_2SO_4, and the solvent was evaporated on a rotary evaporator. The mixture was purified by column chromatography on silica gel eluting with ethyl acetate/*n*-hexane (1:8) to give a bright yellow solid (R_f: 0.2). Yield: 3.4 g (63%). ^{1}H NMR ($CDCl_3$, δ): 7.47 (d, 4H, J = 8.53 Hz), 7.37 (d, 4H, J = 8.54 Hz), 7.30 (d, 4H, J = 8.05 Hz), 7.17 (d, 2H, J = 11.7 Hz), 7.15−7.05 (m, 12H), 6.07 (s, 1H), 6.00 (s, 1H), 3.88 (q, 12H, 7.00 Hz), 1.27 (t, 18H, 7.00 Hz). ^{13}C NMR ($CDCl_3$, δ): 148.50, 148.24, 147.30, 146.40, 135.19, 131.84, 129.37, 127.77, 127.43, 124.84, 124.61, 123.41, 123.13, 115.29, 58.57, 18.30. MS (MALDI-TOF): m/z 864.33 (100%) calcd for $C_{52}H_{60}N_2O_6Si_2$ 864.40 (100%).

Synthesis of TEVS-TPD Polymer. To a solution of TEVS-TPD (**2**) (0.300 g, 0.347 mmol) in THF (2.7 g) were added HCl (35%, 0.38 mg, 10.4 μmol) and water (62.5 mg, 3.47 mmol). The mixture was stirred at 60 °C for 2 h. After being cooled to room temperature, the reaction mixture was diluted with chloroform (20 mL) and washed with water. The organic layer was dried over $MgSO_4$, and the solvent was removed on a rotary evaporator. The product was dried as a yellow powder under a vacuum and stored below 4 °C. Yield: 0.225 g (>95%). M_n = 10 400, M_w = 26 500 (polystyrene standards).

Preparation of Spin-Coated Organosilicate Films on ITO. TEVS-TPD polymer films were obtained by spin-coating the initial polymer solution in chlorobenzene (5 mg/mL, 3500 rpm for the 10 nm thick film; 20 mg/mL, 4000 rpm for the 40 nm thick film) onto clean and UV-ozone treated ITO substrates and subsequent thermal curing at 180 °C for 1 h under argon atmosphere.

For comparison, TEVS-TPD monomer films were prepared from aqueous alcohol solutions adjusted to pH of 4.5 with acetic acid to facilitate cross-linking, as described previously.[22] A solvent for the monomer solutions was comprised of 80% ethanol, 10% H_2O, and 10% chlorobenzene. The monomer solutions of 10 mg/mL (30 mg/mL) were spin-coated at 3000 rpm (2500 rpm) for the films of 10 nm (40 nm) thickness in ambient air followed by in situ thermal curing at 180 °C for 1 h under argon atmosphere. Cross-linked TEPCS-TPD polymer films (see Scheme 2) were prepared from the polymer solutions in the same way (5 mg/mL, 3000 rpm for the 10 nm thick film; 15 mg/mL, 2500 rpm for the 40 nm thick film).

Organic Thin Film Transistor (OTFT) Preparation. The OTFT devices were prepared with the HITL film as the active layer to measure its charge mobility. They were fabricated in bottom-gate/bottom-contact type, where heavily doped silicon substrates were employed as substrate and gate electrodes, thermally grown SiO2, 300 nm, as gate dielectric, and Cr/Au (2 nm/50 nm) as source and drain electrodes. The source and drain electrodes were thermally evaporated and patterned by a lift-off process. Channel lengths of 10 μm were employed in bottom-contact type devices. The active layer was deposited by spin-coating TEVS-TPD polymer solution in chlorobenzene (5 mg/mL, 3000 rpm) followed by in situ thermal curing at 180 °C for 1 h under nitrogen atmosphere. The current−voltage data of the devices were obtained in ambient condition, and the field-effect mobility was estimated from the slope of $I_D^{1/2}$ versus V_G in the saturation regime (transfer characteristic).

OLED Device Fabrication. The solution-processed phosphorescent devices were prepared to investigate TEVS-TPD polymer as a replacement for PEDOT:PSS, as follows. Indium−tin−oxide (ITO) coated glass substrates were cleaned with acetone and isopropyl alcohol and dried in an oven at 200 °C for 5 min. Next, they were treated with a UV-ozone procedure before device fabrication. The organosilicate HITLs were obtained by spin-coating the solutions onto the ITO substrates and subsequently thermally curing at 180 °C for 1 h. The emissive layer (40 nm) was formed via spin-coating a blended solution of poly(vinylcarbazole) (PVK) and *fac*-tris(2-phenylpyridine) iridium(III) ($Ir(ppy)_3$) in chlorobenzene (total 1.5 wt % in chlorobenzene, 6 wt % $Ir(ppy)_3$:PVK). 2,9-Dimethyl-4,7-diphenyl-1,10-phenanthroline (BCP, 10 nm), tris(8-hydroxyquinolinato)aluminum (Alq_3, 40 nm), LiF (1 nm), and Al (100 nm) were deposited as the hole blocking layer, electron transporting layer, and cathode by thermal evaporation at a base pressure of $<5 \times 10^{-7}$ Torr. Next, the device was encapsulated with a glass cap. The device based on PEDOT:PSS was fabricated as the control device, with 40 nm thick PEDOT:PSS (Bayer, Baytron P VP AI 4083) layer spin-coated and subsequently annealed at 200 °C for 5 min.

III. RESULTS AND DISCUSSION

1. Synthesis of TEVS-TPD Monomer and Polymer. *N,N′*-Diphenyl-*N,N′*-bis(4-bromophenyl)biphenyl-4,4′-diamine (TPD-Br2, **1**) was prepared in 68% yield by the Buchwald−Hartwig reaction of 1,4-dibromobenzene and *N,N′*-diphenylbenzidine. The aryl-Br moiety was then directly substituted with vinyltriethoxysilane using mild Heck chemistry to obtain the desired monomer, *N,N′*-diphenyl-*N,N′*-bis(4-((*E*)-2-(triethoxysilyl)vinyl)-phenyl) biphenyl-4,4′-diamine (TEVS-TPD, **2**)[28] (Scheme 1). This procedure to attach triethoxysilane groups is very straightforward, introduces extended conjugation between Si and the aromatic portion, and tolerates many functional groups unlike traditional approaches that use organomagnesium or butyllithium chemistry.[30] Furthermore, the reaction can be performed at room temperature by adjusting the catalyst Pd:P ratio to be 1.0:1.1.[29] The TEVS-TPD polymer was prepared by an acid-catalyzed sol−gel reaction as described previously in >95% yield.[31,32] The molar mass of the synthesized polymer could be carefully adjusted by varying the acid and water content. The number-average molar mass (M_n) and weight-average molar mass (M_w) of TEVS-TPD polymer were 10 400 and 26 500, respectively, as determined by gel permeation chromatography (GPC) calibrated with polystyrene standards. The molar masses of the polymer in chlorobenzene (20 mg/mL) stored for one month in ambient condition were measured to check the stability of the polymer. The values of M_n and M_w of 10 900 and 31 500, respectively, and the GPC curves shown in the Supporting Information demonstrate a good stability of TEVS-TPD polymer in ambient condition.

dx.doi.org/10.1021/ja1061517 |*J. Am. Chem. Soc.* 2011, 133, 1375–1382

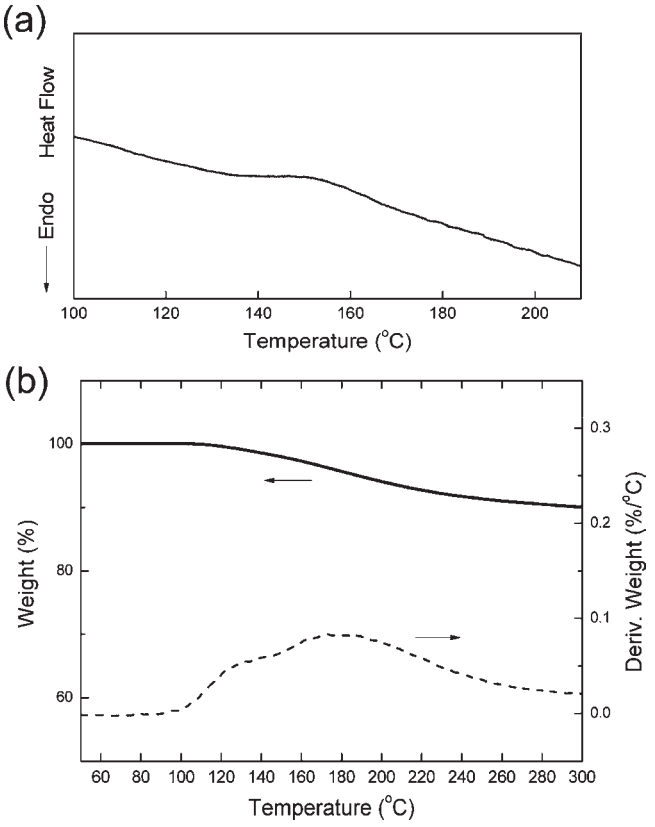

Figure 1. (a) DSC and (b) TGA results of TEVS-TPD polymer obtained with 5 °C/min heating rate.

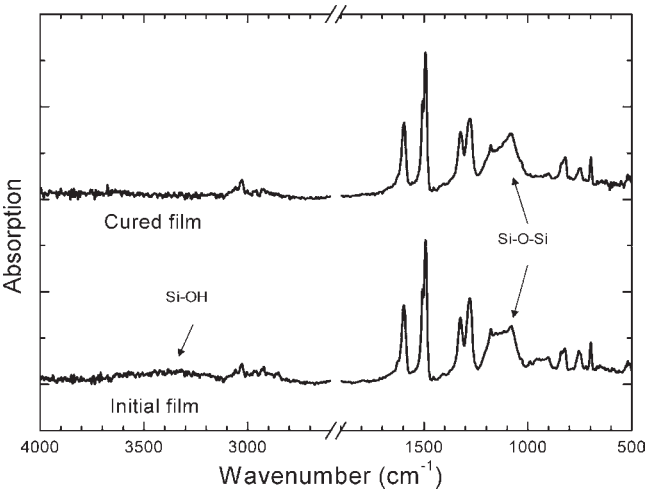

Figure 2. FT-IR spectra of the initial TEVS-TPD polymer film and the cross-linked film prepared by thermal curing at 180 °C for 1 h.

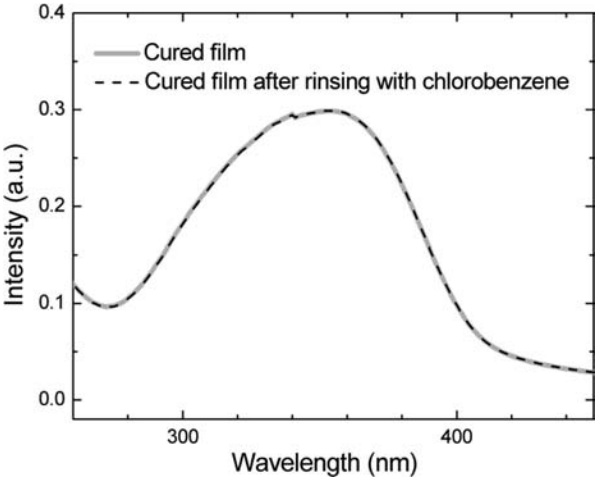

Figure 3. UV−vis absorption spectra of TEVS-TPD polymer films thermally cured at 180 °C for 1 h before (solid) and after rinsing (dash) with chlorobenzene.

The synthetic protocol is simplified to allow for scaling the material synthesis to high volumes as shown in Scheme 1. The key to our process is avoiding pyrophoric chemistry such as *n*-butyl lithium, which is known to be very dangerous for bench chemistry as well as scale-up processes. That is, the final material was prepared in three simple steps from commercially available materials to form a stable polymer powder that can be exposed to ambient conditions without degradation. For example, aliquots can be taken of the solid polymer to prepare solutions as needed, or stock solutions can be prepared and used over extended time periods without detrimental changes. Thus, we anticipate our HITLs to have a much longer shelf life than PEDOT:PSS dispersions that are known to aggregate over time.

2. Characterization of TEVS-TPD Polymer. DSC results of spin-coated and dried TEVS-TPD polymer exhibit a broad exothermic peak between 125 and 175 °C in the first heating, as shown in Figure 1a, which corresponds to the secondary condensation (cross-linking) involving the silanol moieties, and the TGA data show a corresponding weight loss characteristic (Figure 1b). The DSC and TGA results indicate that solvent-resistant cross-linked films can be obtained by carrying out the curing reaction above ca. 175 °C. Therefore, we prepared highly cross-linked TEVS-TPD films by spin-coating the polymer solution in chlorobenzene, followed by in situ thermal cross-linking (curing) at 180 °C for 1 h under nitrogen atmosphere. The secondary condensation reaction of TEVS-TPD polymer films was monitored by FT-IR measurements before and after thermal curing (Figure 2). The absorption signals of the asymmetric Si−O−Si stretch near 1100 cm^{-1} increased after thermal curing due to the secondary condensation reaction involving silanol groups. The thermally cured films showed no visible damage nor any discernible change in the UV−vis spectrum upon exhaustive rinsing with chlorobenzene, a common spin-coating solvent for the emissive layers (Figure 3).

UV−vis absorption and photoluminescence (PL) spectra showed a red-shift after thermal curing, most likely due to the increased film density and closer packing of the chromophores as shown in Figure 4a. The optical band gap of cross-linked TEVS-TPD thin films is 3.0 eV, as determined from the absorption edge of the UV−vis spectrum. Electrochemical characteristics of cross-linked TEVS-TPD on an ITO electrode, investigated by cyclic voltammetry, showed fully reversible electrochemical behavior with no change in the cathodic and anodic peak current upon repeated scans (Figure 4b). This shows that cross-linked TEVS-TPD films have excellent electrochemical stability. The highest occupied molecular orbital (HOMO) energy level is −5.4 eV, and the lowest unoccupied molecular orbital (LUMO) energy level is −2.4 eV, as determined from the cyclic voltammetry and optical band gap. Such a high-lying LUMO energy level is a desired attribute, indicating the capability of TEVS-TPD film to

dx.doi.org/10.1021/ja1061517 |*J. Am. Chem. Soc.* 2011, 133, 1375–1382

function also as an electron blocking layer, which helps to enhance the efficiency of OLEDs and OPVs.

The surface morphology study of cross-linked TEVS-TPD films of 10 and 40 nm thickness, respectively, on ITO substrate was carried out using tapping mode AFM. In addition, a dual layer film of 10 nm thick cross-linked TEVS-TPD layer on top of 40 nm thick PEDOT:PSS film was investigated. The rms roughnesses of the 10 nm and the 40 nm thick cross-linked TEVS-TPD, the dual layer, and PEDOT:PSS films were 2.9, 1.1, 1.8, and 1.5 nm, respectively. After being immersed in chlorobenzene and subsequent drying, the 10 nm thick and the 40 nm thick cross-linked TEVS-TPD and the dual layer films showed decreased rms roughnesses of 1.6, 0.7, and 1.1 nm, respectively (see the Supporting Information). Therefore, the films with cross-linked TEVS-TPD are very smooth as compared to the ITO substrate, whose rms roughness was determined to be 3.0−3.7 nm by AFM, indicating the effective planarization of the ITO surface.

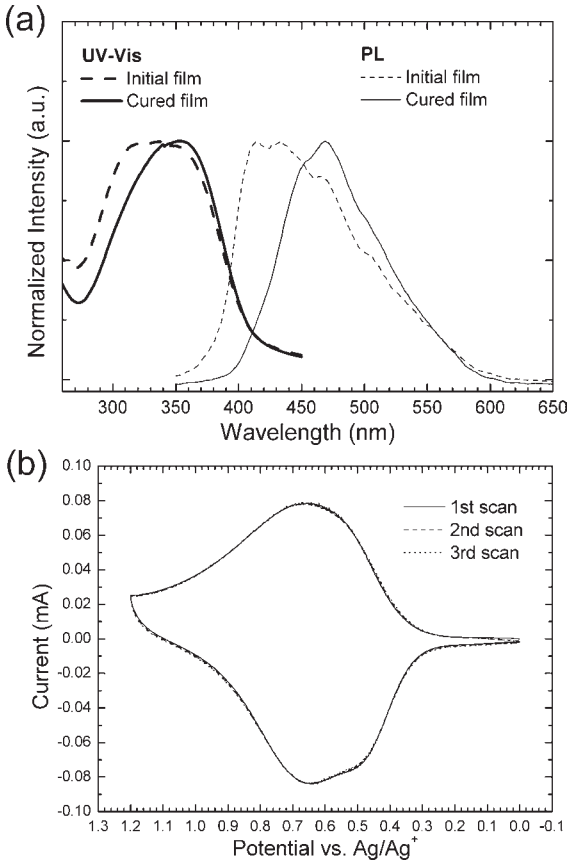

Figure 4. (a) UV−vis absorption (thick) and PL (thin) spectra of the initial TEVS-TPD polymer film (dash) and the cross-linked film (solid) by thermal curing at 180 °C for 1 h. The cured film shows a red-shift in both absorption and emission spectra. (b) Cyclic voltammogram of cross-linked TEVS-TPD on ITO scanned three times to show enhanced electrochemical stability.

Field-effect charge mobility of cross-linked TEVS-TPD was investigated by OTFT measurements. The OTFTs were fabricated with gold bottom contacts, n-doped Si gate, and thermally grown SiO_2 dielectric. Figure 5 shows the transfer and output characteristics of the OTFT device. Cross-linked TEVS-TPD devices exhibited p-channel transistor characteristics with an average field-effect hole mobility of 1.2×10^{-6} $cm^2/(V \cdot s)$. This value is substantially lower than the reported mobility of PEDOT:PSS (10^{-2}−10^{-3} $cm^2/(V \cdot s)$),[33,34] but it is somewhat higher than the reported hole mobility of other triphenylamine (TPA) based, similarly conjugated, vinyl cross-linked polymers ($\sim 10^{-7}$ $cm^2/(V \cdot s)$).[17,34] The mobility is even comparable to TPA-based, fluorene-containing, fully conjugated polymers ($\sim 10^{-6}$ $cm^2/(V \cdot s)$).[34,35] In comparison, inserting nonconjugated moiety between the silicon and the aromatic amine resulted in a significantly decreased mobility too small to be measured by the OTFT characteristics (see below). Therefore, the measured hole mobility of cross-linked TEVS-TPD clearly indicates the importance of having extended conjugation between the silicon atom and the aromatic amine portion in TEVS-TPD.

3. OLED Device Characteristics. In this section, performance characteristics of OLEDs with TEVS-TPD polymer layers of different thicknesses as HITLs are presented. In addition, devices based on the TEVS-TPD monomer and a different organosilicate polymer containing insulating moieties between the Si atom and the aromatic amine moiety are also presented for comparison.

3.1. Characteristics of Devices Based on Cross-linked TEVS-TPD Polymer HITL Layers. To test the performance of the organosilicate polymer as HITLs, solution-processed phosphorescent OLED devices were fabricated using the following device structure: ITO/HITL/6 wt % *fac*-tris(2-phenylpyridine) iridium(III) (Ir(ppy)$_3$):poly(vinyl carbazole) (PVK)/2,9-dimethyl-4,7-diphenyl-1,10-phenanthroline (BCP)/tris(8-hydroxyquinolinato)aluminum

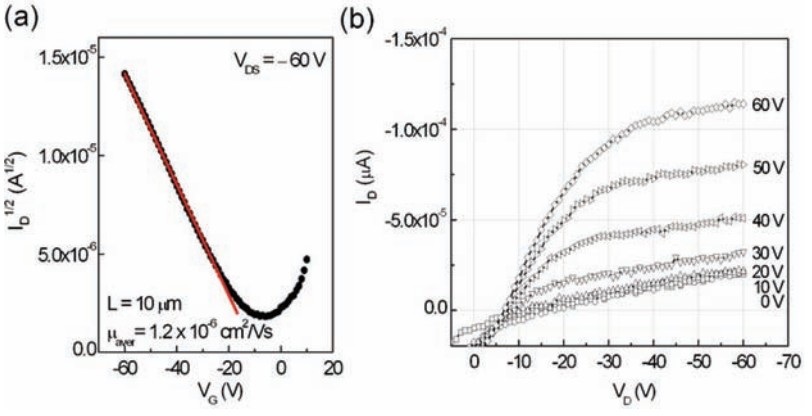

Figure 5. (a) Transfer and (b) output characteristics of OTFT with cross-linked TEVS-TPD polymer film as the active layer. The field-effect mobility calculated in the saturation regime is 1.2×10^{-6} $cm^2/V \cdot s$.

dx.doi.org/10.1021/ja1061517 |J. Am. Chem. Soc. 2011, 133, 1375–1382

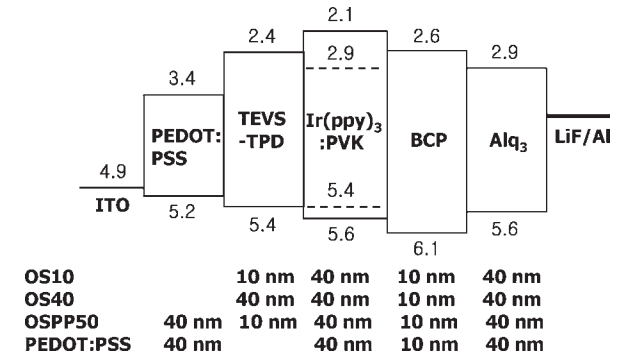

Figure 6. Device structures [ITO/HITL (OS10, OS40, OSPP50, PEDOT:PSS)/Ir(ppy)$_3$:PVK emissive layer (40 nm)/BCP (10 nm)/Alq$_3$ (40 nm)/LiF (1 nm)/Al (100 nm)] and the corresponding energy level diagram. The energy levels of the materials except cross-linked TEVS-TPD are literature values.[36−38]

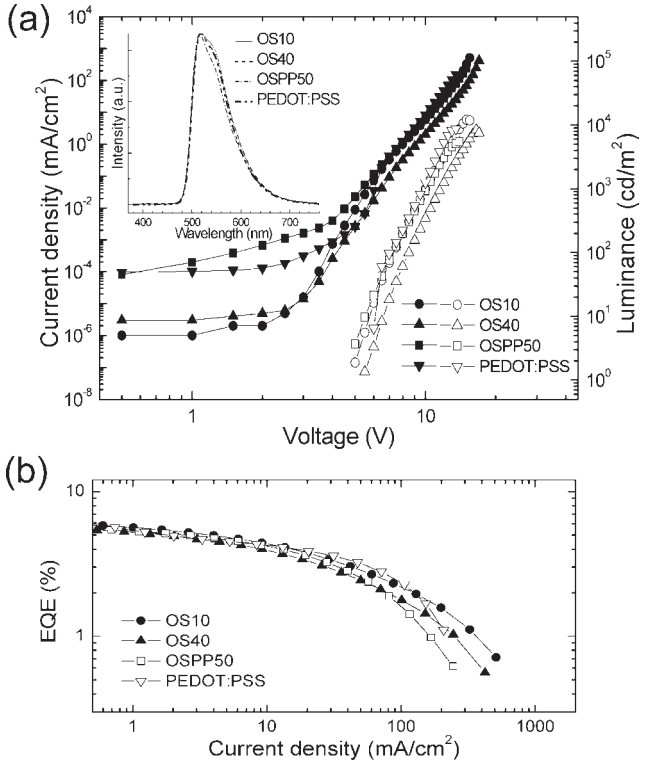

Figure 7. (a) Current density−voltage−luminance characteristics of the OLED devices prepared with cross-linked TEVS-TPD polymer HITLs. The inset is the normalized EL spectra. (b) External quantum efficiency (EQE) versus the current density of the devices.

(Alq$_3$)/LiF/Al. Figure 6 shows the device structures and the corresponding energy diagram schemes.[36−38] The cross-linked TEVS-TPD layers of two different thicknesses, 10 and 40 nm, were employed as HITL layers in preparing the phosphorescent OLED devices, denoted as OS10 and OS40, respectively. For comparison, the control devices were prepared using 40 nm thick PEDOT:PSS as the HITL layer. In addition, devices using a dual HITL layer of 50 nm thickness, comprised of cross-linked TEVS-TPD (10 nm) on top of PEDOT:PSS (40 nm) layer in contact with ITO, were also tested and denoted OSPP50.

The electroluminescence (EL) spectra of the OLED devices exhibit green emission without any emission from the HITLs (Figure 7a, inset), showing that hole/electron recombination occurs in the emissive layer (EML). The important device characteristics are summarized in Table 1. Figure 7 shows the current density−voltage−luminance characteristics (Figure 7a) and the external quantum efficiency (EQE) versus current density (Figure 7b), respectively. As shown in Figure 7a, the devices based on cross-linked TEVS-TPD exhibit a lower leakage current. The turn-on voltages (voltage at 1.0 cd/m^2) of OS10 and OS40 are 5.0 and 5.5 V, respectively, which are lower than the corresponding value, 6.0 V, for the control device with PEDOT:PSS. This is the first time that a single cross-linked polymer HITL layer is shown to successfully exhibit a lower turn-on voltage with lower leakage current than that obtained with PEDOT:PSS. Moreover, the maximum luminance of 12 100 cd/m^2 for OS10 device is greater than 8740 cd/m^2 obtained for the control PEDOT:PSS device. As shown in Table 1, the maximum luminance efficiency (LE), maximum power efficiency (PE), and maximum external quantum efficiency (EQE) of OS10, as compared to the corresponding values for PEDOT:PSS in parentheses, are 22.3 cd/A (22.4 cd/V), 13.5 lm/W (10.1 lm/W), and 6.4% (6.4%) at the current density of 0.10 mA/cm^2 (0.43 mA/cm^2), respectively. The maximum efficiencies of OS10-based devices are comparable to the PEDOT:PSS device. At 1000 cd/m^2, the values of LE and EQE are 16.3 cd/A and 4.7% for OS10, as compared to 14.9 cd/A and 4.2% for the PEDOT:PSS device. Experimental results in Figure 7 and Table 1 show that OS40 devices with thicker (40 nm) TEVS-TPD layer exhibit slightly lower performance characteristics than OS10 (10 nm thickness). It is possibly due to relatively low hole transport in thicker cross-linked TEVS-TPD layer. In comparison, the results for dual HITL layer show results of slightly lower performance than PEDOT:PSS at low current density. Overall, a single thin layer of TEVS-TPD of 10−40 nm thickness seems to provide device performance characteristics superior to those of the dual layer (OSPP50).

3.2. Characteristics of Devices Based on TEVS-TPD Monomer. To investigate the benefits of employing TEVS-TPD polymer, as compared to the corresponding monomer, for use as HITL, we fabricated devices employing TEVS-TPD monomer with the

Table 1. Comparison of Device Characteristics of OLEDs Prepared with Various Cross-linked TEVS-TPD Polymer HITLs

	V_{on} (V)[a]	max L (cd/m^2)[b]	V_B (V)[c]	LE$_{max}$ (cd/A)[d]	PE$_{max}$ (lm/W)[e]	EQE$_{max}$ (%)[f]	EQE$_{1000}$ (%)[g]
OS10	5.0	12 090	15.0	22.3	13.5	6.4	4.7
OS40	5.5	8350	16.5	20.0	11.4	6.2	4.3
OSPP50	5.0	5500	14.0	18.8	10.3	5.5	4.5
PEDOT:PSS	6.0	8740	13.5	22.4	10.1	6.4	4.3

[a] Turn-on voltage. [b] Maximum luminance. [c] Voltage at maximum luminance. [d] Maximum luminance efficiency. [e] Maximum power efficiency. [f] Maximum external quantum efficiency (EQE). [g] EQE at 1000 cd/m^2.

dx.doi.org/10.1021/ja1061517 |J. Am. Chem. Soc. 2011, 133, 1375–1382

Table 2. Device Characteristics of OLEDs Prepared with Various Cross-linked TEVS-TPD Monomer HITLs

	V_{on} (V)[a]	max L (cd/m^2)[b]	V_B (V)[c]	LE_{max} (cd/A)[d]	PE_{max} (lm/W)[e]	EQE_{max} (%)[f]	EQE_{1000} (%)[g]
(OS10)	(5.0)	(12 090)	(15.0)	(22.3)	(13.5)	(6.4)	(4.7)
OSM10	6.0	11 580	14.0	15.1	6.6	4.3	3.8
OSM40	6.0	10 970	14.0	13.8	5.9	4.0	3.6
OSMPP50	5.0	7890	12.0	11.4	5.1	3.4	2.2

[a] Turn-on voltage. [b] Maximum luminance. [c] Voltage at maximum luminance. [d] Maximum luminance efficiency. [e] Maximum power efficiency. [f] Maximum external quantum efficiency (EQE). [g] EQE at 1000 cd/m^2.

Table 3. Device Characteristics of OLEDs Prepared with Various Cross-linked TEPCS-TPD Polymer HITLs

	V_{on} (V)[a]	max L (cd/m^2)[b]	V_B (V)[c]	LE_{max} (cd/A)[d]	PE_{max} (lm/W)[e]	EQE_{max} (%)[f]	EQE_{1000} (%)[g]
(OS10)	(5.0)	(12 090)	(15.0)	(22.3)	(13.5)	(6.4)	(4.7)
OSI10	7.5	6200	15.0	14.1	4.6	4.1	3.4
OSI40	8.5	2070	17.0	20.1	7.1	5.8	3.0
OSPPI50	6.5	7440	16.5	15.3	6.9	4.5	2.9

[a] Turn-on voltage. [b] Maximum luminance. [c] Voltage at maximum luminance. [d] Maximum luminance efficiency. [e] Maximum power efficiency. [f] Maximum external quantum efficiency (EQE). [g] EQE at 1000 cd/m^2.

same device structure. TEVS-TPD monomer layers were prepared from aqueous alcohol solutions with pH = 4.5 in a solvent of 80% ethanol, 10% H_2O, and 10% chlorobenzene to facilitate cross-linking.[22] The characteristics of solvent resistance and film morphology of thermally cured films (180 °C for 1 h) are inferior to those of the corresponding films prepared from the TEVS-TPD polymer (Supporting Information). HITLs of TEVS-TPD monomer of 10 and 40 nm thickness were deposited by spin-coating followed by thermal curing at 180 °C for 1 h, denoted as OSM10 and OSM40. Devices employing a dual layer of 10 nm thick TEVS-TPD monomer layer on PEDOT:PSS as HITL were also prepared and denoted as OSMPP50. Table 2 summarizes their device characteristics as compared to those of the device based on TEVS-TPD polymer layer of 10 nm thickness (OS10); the full details are shown in the Supporting Information. The devices employing TEVS-TPD monomer HITLs (OSM) show significantly deteriorated device performances and higher leakage current as compared to the devices using cross-linked TEVS-TPD polymer HITLs (OS10), most likely due to the inferior solvent resistance and film morphology.

3.3. Characteristics of Devices Based on an Organosilicate Polymer Containing Insulating Moiety between Si and Aromatic Amine. To investigate the effects of having extended conjugation between the Si atom and the aromatic amine moiety in TEVS-TPD polymer due to the vinyl link, a different organosilicate containing the aromatic amine TPD and insulating moiety, *N*,*N*′-bis(4-*n*-butylphenyl)-*N*,*N*′-bis[4-{3-(triethoxysilyl)propyl}-carbamoyloxymethylphenyl]-1,1′-biphenyl-4,4′-diamine (TEPCS-TPD), was prepared. Scheme 2 shows the structure of the TEPCS-TPD monomer, and its synthesis and polymerization is described in the Supporting Information. The thermally cured (at 180 °C for 1 h) TEPCS-TPD polymer samples showed excellent solvent resistance (i.e., no change in UV−vis spectrum after rinsing in various solvents) and good film morphology as shown in the Supporting Information. OLED devices were prepared with cross-linked TEPCS-TPD polymer layers of 10 and 40 nm thickness, and a dual layer of 10 nm thick cross-linked TEPCS-TPD polymer layer on PEDOT:PSS as HITLs, denoted as OSI10, OSI40, and OSIPP50, respectively. The device performance characteristics are summarized in Table 3 as compared to those of 10 nm thick TEVS-TPD polymer (OS10). The turn-on voltages are higher, and the efficiencies of the devices are significantly lower than those of the TEVS-TPD polymer HITLs. This result is most likely due to a very low hole mobility of TEPCS-TPD polymer films, because the OTFT devices with cross-linked TEPCS-TPD as the active layer did not exhibit any measurable field-effect mobility.

IV. CONCLUSIONS

A thermally cross-linkable, TEVS-TPD organosilicate polymer with aromatic amine functionality was prepared under mild conditions via sequential Heck and sol−gel chemistry to obtain a highly cross-linked HITL thin film by spin-coating, followed by in situ thermal curing. In addition to the mild synthetic process, important to our process is the extended conjugation introduced between the silicon atom and the aromatic amine portion of the material by employing a vinylsiloxane linkage, which leads to an enhanced hole mobility as compared to the traditional alkylsiloxane linkage. In initial tests with solution-processed phosphorescent OLEDs, the devices with cross-linked TEVS-TPD HITL (10 nm thickness) exhibited lower turn-on voltage with lower leakage current, higher luminance and stability at high current density, and similar maximum efficiencies at low voltages as compared to those based on PEDOT:PSS HITL. In addition, the devices based on cross-linked TEVS-TPD exhibited device performances superior to those of the devices prepared with TEVS-TPD monomer or TEPCS-TPD polymer that contains insulating moieties between the silicon atom and the aromatic amine. To test the general applicability of the highly conjugated organosilicate polymers in organic electronic devices, further tests with other OLED structures and OPVs employing cross-linked TEVS-TPD type HITLs are currently under investigation. It is anticipated that the interface between the active organic layer and our new HITLs (in OLEDs and OPVs) will be much more mild than with the corresponding corrosive PEDOT:PSS, leading to devices with improved device performance and lifetime.[6,39] Last, we anticipate our HITLs to have a much longer shelf life than PEDOT:PSS dispersions that are known to aggregate over time.

■ ASSOCIATED CONTENT

Supporting Information. Description of synthesis and characterization of the materials, AFM images of HITL films, and

dx.doi.org/10.1021/ja1061517 |*J. Am. Chem. Soc.* 2011, 133, 1375–1382

additional device results. This material is available free of charge via the Internet at http://pubs.acs.org.

AUTHOR INFORMATION

Corresponding Author
dyyoon@snu.ac.kr; jjkim@snu.ac.kr; aselli@stanford.edu

ACKNOWLEDGMENT

This research was supported by the Division of Chemistry and Molecular Engineering of Brain Korea 21 Program and the OLED Center at Seoul National University. It was in part supported by the Korea−Germany International Research Training (IRTG) grant from the National Research Foundation of Korea.

REFERENCES

(1) de Jong, M. P.; van Ijzendoorn, L. J.; de Voigt, M. J. A. *Appl. Phys. Lett.* **2000,** *77*, 2255.
(2) Wong, K. W.; Yip, H. L.; Luo, Y.; Wong, K. Y.; Lau, W. M.; Low, K. H.; Chow, H. F.; Gao, Z. Q.; Yeung, W. L.; Chang, C. C. *Appl. Phys. Lett.* **2002,** *80*, 2788.
(3) Nguyen, T. P.; de Vos, S. A. *Appl. Surf. Sci.* **2004,** *221*, 330.
(4) Lee, J. Y. *Synth. Met.* **2006,** *156*, 537.
(5) Kim, J.-S.; Ho, P. K. H.; Murphy, C. E.; Seeley, A. J. A. B.; Grizzi, I.; Burroughes, J. H.; Friend, R. H. *Chem. Phys. Lett.* **2004,** *386*, 2.
(6) Kim, J.-S.; Friend, R. H.; Grizzi, I.; Burroughes, J. H. *Appl. Phys. Lett.* **2005,** *87*, 023506.
(7) Bacher, E.; Bayerl, M.; Rudati, P.; Reckefuss, N.; Müller, C. D.; Meerholz, K.; Nuyken, O. *Macromolecules* **2005,** *38*, 1640.
(8) Bellmann, E.; Shaheen, S. E.; Thayumanavan, S.; Barlow, S.; Grubbs, R. H.; Marder, S. R.; Kippelen, B.; Peyghambarian, N. *Chem. Mater.* **1998,** *10*, 1668.
(9) Bacher, A.; Erdelen, C. H.; Paulus, W.; Ringsdorf, H.; Schmidt, H.-W.; Schuhmacher, P. *Macromolecules* **1999,** *32*, 4551.
(10) Jungermann, S.; Riegel, N.; Müller, D.; Meerholz, K.; Nuyken, O. *Macromolecules* **2006,** *39*, 8911.
(11) Domercq, B.; Hreha, R. D.; Zhang, Y.-D.; Larribeau, N.; Haddock, J. N.; Schultz, C.; Marder, S. R.; Kippelen, B. *Chem. Mater.* **2003,** *15*, 1491.
(12) Liu, S.; Jiang, X.; Ma, H.; Liu, M. S.; Jen, A. K.-Y. *Macromolecules* **2000,** *33*, 3514.
(13) Lim, B.; Hwang, J.-T.; Kim, J. Y.; Ghim, J.; Vak, D.; Noh, Y.-Y.; Lee, S.-H.; Lee, K.; Heeger, A. J.; Kim, D.-Y. *Org. Lett.* **2006,** *8*, 4703.
(14) Niu, Y.-H.; Liu, M. S.; Ka, J.-W.; Jen, A. K.-Y. *Appl. Phys. Lett.* **2006,** *88*, 093505.
(15) Liu, M. S.; Niu, Y.-H.; Ka, J.-W.; Yip, H.-L.; Huang, F.; Luo, J.; Kim, T.-D.; Jen, A. K.-Y. *Macromolecules* **2008,** *41*, 9570.
(16) Ma, B.; Lauterwasser, F.; Deng, L.; Zonte, C. S.; Kim, B. J.; Fréchet, J. M. J.; Borek, C.; Thompson, M. E. *Chem. Mater.* **2007,** *19*, 4827.
(17) Paul, G. K.; Mwaura, J.; Argun, A. A.; Taranekar, P.; Reynolds, J. R. *Macromolecules* **2006,** *39*, 7789.
(18) Niu, Y.-H.; Liu, M. S.; Ka, J.-W.; Bardeker, J.; Zin, M. T.; Schofield, R.; Chi, Y.; Jen, A. K.-Y. *Adv. Mater.* **2007,** *19*, 300.
(19) Cheng, Y.-J.; Liu, M. S.; Zhang, Y.; Niu, Y.; Huang, F.; Ka, J.-W.; Yip, H.-L.; Tian, Y.; Jen, A. K.-Y. *Chem. Mater.* **2008,** *20*, 413.
(20) Yan, H.; Lee, P.; Armstrong, N. R.; Graham, A.; Evmenenko, G. A.; Dutta, P.; Marks, T. J. *J. Am. Chem. Soc.* **2005,** *127*, 3172.
(21) Yan, H.; Huang, Q.; Scott, B. J.; Marks, T. J. *Appl. Phys. Lett.* **2004,** *84*, 3873.
(22) Li, J.; Marks, T. J. *Chem. Mater.* **2008,** *20*, 4873.
(23) Huang, Q.; Li, J.; Marks, T. J.; Evmenenko, G. A.; Dutta, P. *J. Appl. Phys.* **2007,** *101*, 093101.
(24) Huang, Q.; Li, J.; Evmenenko, G. A.; Dutta, P.; Marks, T. J. *Chem. Mater.* **2006,** *18*, 2431.
(25) Huang, Q.; Evmenenko, G. A.; Dutta, P.; Lee, P.; Armstrong, N. R.; Marks, T. J. *J. Am. Chem. Soc.* **2005,** *127*, 10227.
(26) Huang, Q.; Evmenenko, G.; Dutta, P.; Marks, T. J. *J. Am. Chem. Soc.* **2003,** *125*, 14704.
(27) Cui, J.; Huang, Q.; Veinot, J. C. G.; Yan, H.; Wang, Q.; Hutchison, G. R.; Richter, A. G.; Evmenenko, G.; Dutta, P.; Marks, T. J. *Langmuir* **2002,** *18*, 9958.
(28) Wahab, M. A.; Sudhakar, S.; Yeo, E.; Sellinger, A. *Chem. Mater.* **2008,** *20*, 1855.
(29) Littke, A. F.; Fu, G. C. *J. Am. Chem. Soc.* **2001,** *123*, 6989.
(30) Shea, K. J.; Loy, D. A. *Chem. Mater.* **2001,** *13*, 3306.
(31) Lee, J,-K.; Char, K.; Rhee, H.-W.; Ro, H. W.; Yoo, D. Y.; Yoon, D. Y. *Polymer* **2001,** *42*, 9085.
(32) Dong, H.; Brook, M. A.; Brennan, J. D. *Chem. Mater.* **2005,** *17*, 2807.
(33) Bernards, D. A.; Malliaras, G. G. *Adv. Funct. Mater.* **2007,** *17*, 3538.
(34) The mobilities in refs 17, 33, and 35 were obtained from space charge limited current (SCLC) hole-only devices, which yield mobility values somewhat different from the values obtained from thin film transistor (TFT) characteristics as employed in this study. The relationship between the SCLC mobility and the TFT mobility can be found from a reference: Pasveer, W. F.; Cottaar, J.; Tanase, C.; Coehoorn, R.; Bobbert, P. A.; Blom, P. W. M.; de Leeuw, D. M.; Michels, M. A. J. *Phys. Rev. Lett.* **2005,** *94*, 206601.
(35) Craciun, N. I.; Wildeman, J.; Blom, P. W. M. *J. Phys. Chem. C* **2010,** *114*, 10559.
(36) Xia, H.; Li, M.; Lu, D.; Zhang, C.; Xie, W.; Liu, W.; Yang, B.; Ma, Y. *Adv. Funct. Mater.* **2007,** *17*, 1757.
(37) Shi, M.-M.; Lin, J.-J.; Shi, Y.-W.; Ouyang, M.; Wang, M.; Chen, H.-Z. *Mater. Chem. Phys.* **2009,** *115*, 841.
(38) Kang, J.-W.; Lee, D.-S.; Park, H.-D.; Park, Y.-S.; Kim, J. W.; Jeong, W.-I.; Yoo, K.-M.; Go, K.; Kim, S.-H.; Kim, J.-J. *J. Mater. Chem.* **2007,** *17*, 3714.
(39) Yamanari., T.; Taima, T.; Sakai, J.; Tsukamoto, J.; Yoshida, Y. *Jpn. J. Appl. Phys.* **2010,** *49*, 01AC02.